

# 带肋矩形直通道内的冷却空气换热特性研究

刘 锐 税琳棋 王新军 白晓伟  
(西安交通大学 叶轮机械研究所 陕西 西安 710049)

**摘 要:** 采用 ANSYS CFX 商用软件对带肋矩形直通道内的冷却空气换热特性进行了数值计算, 并与文献 [4] 的实验数据进行了对比, 分析了雷诺数  $Re$  和肋片角度对努塞尔特数  $Nu$  的影响。结果表明:  $Nu$  数计算平均值与实验值的变化趋势一致, 但计算结果大于实验值; 由于肋片的扰流作用, 在两个肋片之间的壁面区域产生了两个旋涡, 强化了冷却空气与固体壁面的换热; 随着  $Re$  数的增大,  $Nu$  数增大, 平均摩擦阻力系数也增大; 当肋片角度在  $45^\circ \sim 60^\circ$  之间时, 冷却通道的强化对流换热效果最好。

**关 键 词:** 叶片冷却; 矩形通道; 流动与换热

中图分类号: TK471 文献标识码: A

## 引 言

现代燃气透平叶片内部一般应用肋片强化传热。针对带肋通道的空气冷却换热问题的研究大部分采用单一的方式, 缺乏实验数据和数值计算结果的对比, 对研究的结果只是进行现象性的描述, 缺乏机理上的分析<sup>[1-4]</sup>。本研究采用 ANSYS CFX 商用软件对带肋矩形通道内空气的流动与换热问题进行计算, 将计算结果与相关实验数据对比来验证结果的合理性, 并从流动和传热的机理上对计算结果进行了深入的分析。研究结果对实际透平叶片内冷却通道结构设计有一定的指导意义。

## 1 计算模型及数据处理

### 1.1 计算模型

计算对象为文献 [4] 的实验通道, 如图 1 所示。通道结构参数: 正方形直通道, 截面尺寸  $51 \text{ mm} \times 51 \text{ mm}$ , 长  $L = 268 \text{ mm}$ , 肋高  $e = 2.4 \text{ mm}$ , 通道当量直径  $D = 51 \text{ mm}$ , 肋间距  $p = 24 \text{ mm}$ , 肋高与当量直径之比

$e/D = 0.047$ , 肋片间距与肋高比  $p/e = 10$ 。

采用 ANSYS CFX 商用软件, 湍流模型为标准  $k-\varepsilon$  湍流模型; 多块结构化网格, 网格在贴壁面处加密, 边界层内壁面法向方向布置不少于 20 个节点, 第一层网格距离壁面  $0.001 \text{ mm}$ , 控制壁面第一层网格的  $y^+$  值不大于 0.2; 网格节点数约为 410 万, 总体计算为二阶精度; 收敛标准为压力及 3 个方向速度分量的均方根残差均小于  $1 \times 10^{-6}$ 。

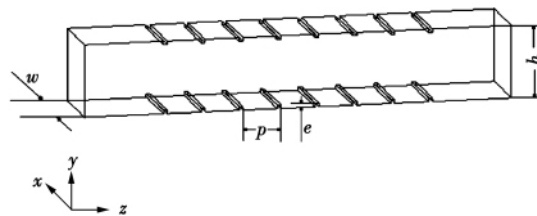


图 1 数值计算模型

Fig. 1 Numerical calculation model

计算边界条件同文献 [4] 实验条件, 冷却工质为空气。绝对坐标系下给定通道进口流速和总温, 出口静压, 通道壁面为无滑移边界条件, 换热条件为均匀热流量。

### 1.2 数据处理

当量直径的定义:

$$D = 2hw / (h + w) \quad (1)$$

式中:  $h, w$ —内冷通道的高度和宽度。

内冷通道  $Re$  数、平均  $Nu$  数的定义:

$$Re = \frac{UD}{\nu}, Nu = \frac{h_0 D}{\lambda} \quad (2)$$

式中:  $\nu$ —按冷却工质进出口平均温度计算的运动粘度;  $U$ —入口平均速度;  $D$ —内冷通道的当量直径;  $h_0$ —按光通道面积计算的平均换热系数;  $\lambda$ —冷却

收稿日期: 2010-10-11; 修订日期: 2010-11-23

基金项目: 国家重点基础研究发展计划 (973 计划) 基金资助项目 (2007CB707701)

作者简介: 刘 锐 (1987-), 男, 湖北仙桃人, 西安交通大学硕士研究生。

工质的导热系数。

## 2 计算结果与分析

### 2.1 Re 数对 Nu 数的影响

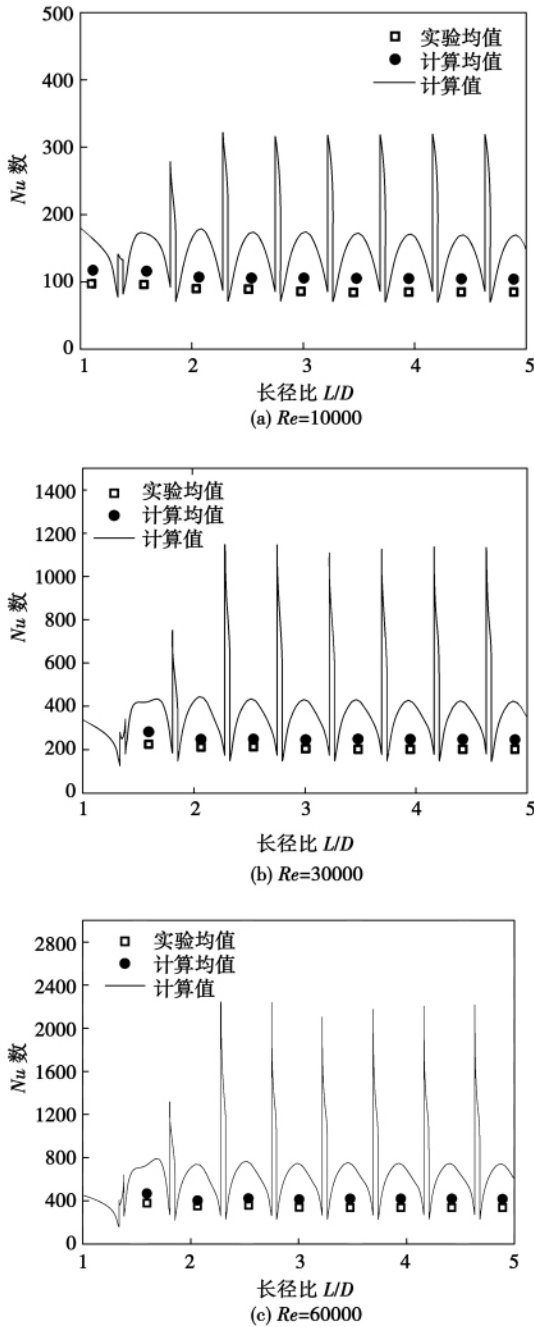


图 2 Re 数对 Nu 数的影响

Fig. 2 The influence of Reynolds number on Nu

图 2 是 3 种雷诺数下  $90^\circ$  直肋冷却通道内壁面 Nu 数的计算值与实验值的比较曲线。可以看出: (1) 相邻两肋之间的计算平均 Nu 数与实验值的变化趋势一致; (2) 在 3 种 Re 下, 当相对距离  $L/D$

$D > 3$  时冷却通道内的流动与换热达到充分发展阶段, 通道内壁面两肋间的流动与换热都趋于相同, 呈现周期性变化; (3) 随着 Re 数的增大, 冷却气流速度增大, 有利于通道内壁面的强化换热, 相应的 Nu 也增大; (4) 由于肋片的扰流作用, 强化了冷却空气与固体壁面的换热强度, 使肋片处的 Nu 数急剧增大。

肋片的强化换热机理可由边界层理论来解释: 当流体流过固体壁面时, 在壁面上就会形成一个流动边界层, 边界层里的流速和温度变化剧烈, 对流换热的热阻也集中在这里。边界层分为 3 层: 层流底层、过渡层和湍流层。在层流底层中, 近壁处的流体几乎不动, 热量的传递依靠流体的导热进行, 流体的导热系数很低, 这就使层流底层中的传热效率远低于湍流核心区的传热效率。在湍流层, 由于流体剧烈混合并充满了旋涡, 温度梯度较小, 热量的传递依靠流体的对流进行。在过渡层, 热传导和对流换热均起作用。

图 3 和图 4 分别显示了 3 种雷诺数下的相对误差分布和平均相对误差随雷诺数的变化规律。结果显示: (1) 各种情况下  $L/D < 3$  时相对误差上下震荡,  $L/D > 3$  误差趋于稳定, 这和图 2 中得出的  $L/D > 3$  时冷却通道内的流动与换热达到充分发展的结论相一致。 (2) 计算结果大于实验值, 其相对偏差约为 17%, 这主要是由于文献 [5] 中实验数据本身存在约 8% 的误差, 同时数值计算模型也会带来一定的误差。 (3) 雷诺数的变化对相对误差的影响可以忽略, 这是由于本研究计算条件都已处在旺盛的湍流区, 所以相对误差对雷诺数变化并不敏感, 和实际情况是一致的。

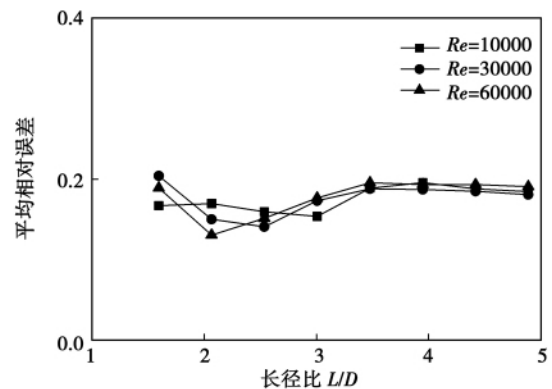


图 3 3 种 Re 数下的相对误差分布

Fig. 3 Relative error distribution under different Reynolds numbers

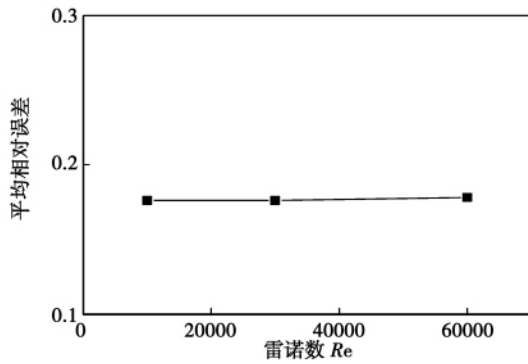


图 4 平均相对误差随  $Re$  数的变化  
Fig. 4 Average relative error changing with Reynolds number

在透平叶片内冷却通道中,冷却工质在通道内流动时受到肋片的限制,使通道内近壁处冷却工质发生分离,增加了近壁区冷却工质的湍流度,使近壁面及肋片间冷却工质的相对速度提高,减薄了流动和传热边界层的厚度,降低了传热热阻,提高了传热系数。肋片主要以两种方式改变了内冷通道中冷却工质的流动结构:一是肋片对冷却工质流动的限制作用,使其在通道内产生分离流动;二是肋片对流体所起的扰流作用,在冷却通道内壁面上按一定间距周期性布置的肋片,使壁面上及肋片间流体边界层得不到充分稳定发展,从而强化冷却工质与固体壁面的换热强度。

### 2.2 肋片角度对 $Nu$ 数的影响

在  $Re = 30000$  条件下,计算了 4 种肋片角度 ( $90^\circ$ 、 $60^\circ$ 、 $45^\circ$  和  $30^\circ$ ) 对冷却通道换热  $Nu$  数的影响并与实验数据进行了比较,如图 2(b) 和图 5 所示。可以看出:(1) 计算平均  $Nu$  数与实验值的变化趋势是一致的,但计算结果与实验值存在一定的偏差  $60^\circ$  和  $45^\circ$  肋片的偏差约为 20%,  $30^\circ$  肋片的偏差约为 10%。(2) 肋片角度的改变引起了通道内冷却空气的流动与传热特性变化,在通道充分发展阶段 ( $L/D > 3$ ),肋片为  $90^\circ$  时的  $Nu$  数约为 240,肋片为  $60^\circ$  和  $45^\circ$  时的  $Nu$  数约为 300,肋片为  $30^\circ$  时的  $Nu$  数约为 250。显然,肋片角度在  $45^\circ \sim 60^\circ$  之间的强化对流换热效果最好,但同时计算误差也最大。原因是斜置肋片与主流呈现一定的角度,将引起二次流,当肋片角度在  $45^\circ \sim 60^\circ$  时,二次流动最为强烈。强化了肋片的扰流作用,显著增加了换热效果。同时由于二次流和主流的混合引起的质量和能量的交换以及二次流对流动造成的扰动,导致数值计算的结果出现偏差。

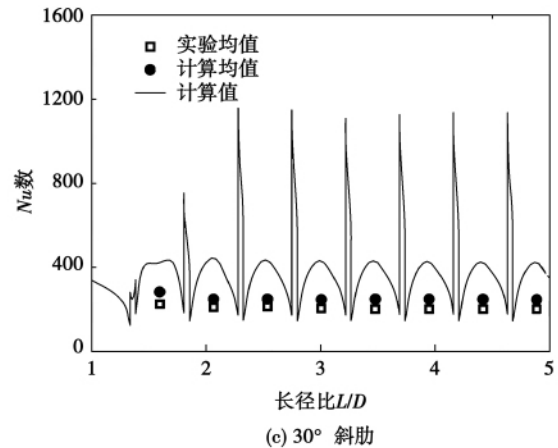
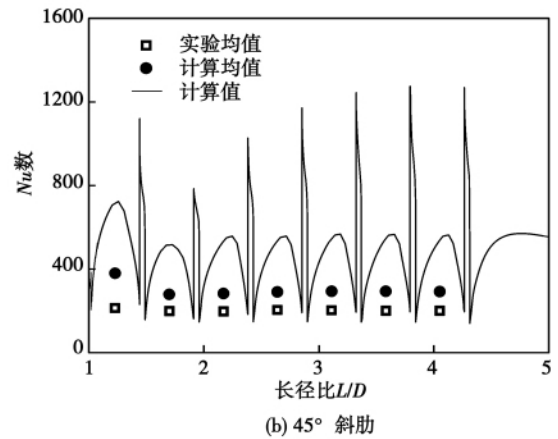
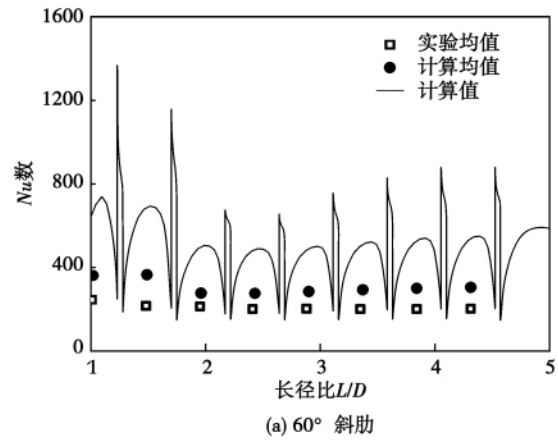


图 5 肋片角度对  $Nu$  数的影响  
Fig. 5 The effect of rib angle on the Nusselt number

### 3 冷却通道内的流场分析

计算模型如图 1 所示。冷却工质为空气,设置通道的进口条件为给定流量和总温,出口条件给定静压,通道内壁面为相同的均匀热流密度  $25 \text{ kW/m}^2$ ,图 6 是进口流量为  $0.03 \text{ kg/s}$  时冷却通道内的速度分布云图和轨迹图。

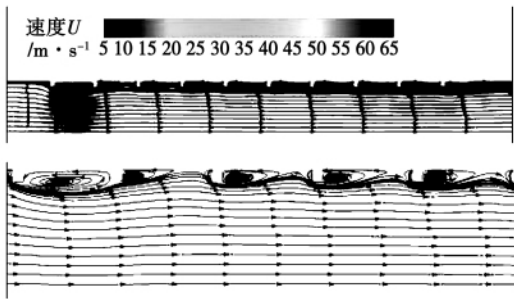


图 6 冷却通道内空气的速度分布和轨迹  
Fig. 6 Trajectories and cloud atlas of velocity in cooling channel

可以看出,通道内壁面附近的流体经过肋片时,由于肋片的扰流作用,在两个肋片之间的内壁面区域产生了两个旋涡。沿流向看,第一个旋涡存在于前面肋片的下游,第二个旋涡存在于下一个肋片的上游,在两个肋片的内壁面中间区为边界层的再附着区域。相对于光滑的内壁面,肋片的作用造成了内壁面附近流体的分离而使得流动紊乱程度加剧,破坏了流动在贴壁面附近的边界层,进而使内壁面流动分离区域与边界层再附着区域流体与通道内主流的换热得到加强,从而提高传热系数。图 6 中左侧第一个肋片下游存在一个较大的旋涡,这是由通道的进口效应产生的;从第三个肋片开始,肋片上下游的流动呈现周期性的两个旋涡;至于肋片的顶部,由于肋片上游存在旋涡,此旋涡的外围分离流体一直延伸至肋片的顶部,这样肋片顶部区域的流体很难在其壁面发展附面边界层,进而肋片顶部区域的换热将势必得到强化。

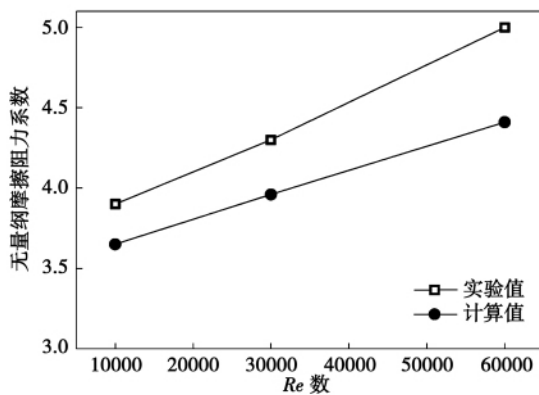


图 7 不同  $Re$  数下的摩擦阻力系数比  
Fig. 7 The average friction coefficient ratio under different Reynolds numbers

从图 6 还可以清楚地看到,肋片的扰流在通道内的影响范围大致为肋片高度  $e$  的 1.5 倍贴壁面区域,通道中间的大部分主流流体呈现出二维流动特性,由此可知肋片的设置不会带来流道内太大的压力损失。图 7 给出了不同雷诺数下带肋与光滑通道内总体平均摩擦阻力系数的比值曲线。可以看出,计算结果与实验值的变化趋势一致,随着  $Re$  的增大,平均摩擦阻力系数比值也增大;计算结果小于实验结果约 11%。

#### 4 结 论

采用商用软件对带肋矩形直通道内的空气流动与换热特性进行了数值研究,分析了  $Re$  和肋片角度对  $Nu$  的影响并与实验数据进行了对比,探讨了冷却通道内流场的特点,得到以下结论:

- (1) 数值计算平均  $Nu$  与实验值的变化趋势一致,但计算结果大于实验值,存在一定偏差。表明数值计算模型和方法仅可以定性研究内冷却通道的换热特性。
- (2) 由于肋片的扰流作用,在两个肋片之间的内壁面区域产生了两个旋涡,强化了冷却空气与固体壁面的换热强度。
- (3) 随着  $Re$  的增大,  $Nu$  增大,平均摩擦阻力系数也增大;当肋片角度在  $45^\circ \sim 60^\circ$  之间时,冷却通道的强化对流换热效果最好。

#### 参考文献:

- [1] IACOVIDES H. Computation of flow and heat transfer through rotating ribbed passage [J]. International Journal of Heat fluid flow, 1998, 393 ~ 400.
- [2] IACOVIDES H, RAISEE M. Recent progress in the computation of flow and heat transfer in internal cooling passages of turbine blades [J]. International Journal of Heat fluid flow, 1999, 320 ~ 328.
- [3] 李广超, 张 魏. 肋角度对矩形通道壁面换热影响的研究 [J]. 汽轮机技术, 2007, 49(3): 202 ~ 205.  
LI Guang-chao, ZHANG Wei. Influence of the rib angle on the heat transfer in the rectangular passage [J]. Turbine technology, 2007, 49(3): 202 ~ 205.
- [4] HAN J C. Heat transfer and friction characteristics in rectangular channels with rib turbulators [J]. ASME Journal of heat transfer, 1988, 110: 321 ~ 328.

( 陈 滨 编 辑 )

engine with the maximal power output of the cycle serving as the optimization target and the heat conduction between the working medium and the external heat channel abiding by the law of radiation-based heat conduction [ $q \propto \Delta(T^n)$ ]. A numerical calculation case was given under the law of radiation-based heat conduction and compared with the results obtained under the Newton's heat law. The results of the numerical calculation case show that with an increase of the heat conductivity, the power output and efficiency of the optimal full and semi cycle will decrease. Compared with the full cycle, the compression ratio, power output and efficiency of the optimal semi-cycle are relatively big. Although the Euler-Lagrange ( $E-L$ ) arc sections and the curves showing the change of the volume of the working medium with time are all similar to sine curves and composed of three sections under both heat conduction laws, the curves showing the change of the volume of the working medium under different heat conduction laws are not a same one. **Key words:** finite-time thermodynamics, law of radiation-based heat conduction, maximal power output, external combustion engine

气液两相流流型图像信息熵递归特性分析 = **Analysis of the Image Information Entropy Recurrence Characteristics of a Gas-liquid Two-phase Flow Pattern** [刊 汉] HONG Wen-peng, LIU Yan, ZHOU Yun-long (College of Energy Source and Power Engineering, Northeast University of Electric Power, Jilin, China, Post Code: 132012) // Journal of Engineering for Thermal Energy & Power. - 2011, 26(5). - 538 ~ 542

By using a high speed video camera, acquired were the flow images of various flow patterns of two kinds of tube bundle in 10 rows and 4 columns with a pitch of 1.3 and 1.8 respectively. In the light of the typical flow images in three types, namely bubble-shaped flow, intermittent flow and mist flow, the information entropy sequence of the various flow pattern images was extracted and the dynamic characteristics of various flow patterns of the gas-liquid two-phase flow and the entropy sequence of the transit flow patterns were studied by using the recurrence analytic method. The research results show that the recurrence structures of the entropy sequences of different flow pattern images are different. The recurrence chart of the information entropy sequence of the bubble-shaped flow images is of a dot-shaped structure, that of the intermittent flow images is of a dot-block-shaped structure while that of the mist flow is of a clearest diagonal structure. The recurrence structures of the entropy sequences of transit flow pattern images can clearly show the evolvement of the transition process of the flow patterns. The recurrence structure chart of information entropy sequence can reflect relatively well the evolvement mechanism of the flow patterns and the recurrence characteristic variable is susceptible to the change of converted flow speed, thus providing a relatively effective method for studying the mechanism governing the flow patterns of gas-liquid two-phase flow. **Key words:** gas-liquid two-phase flow, tube bundle, flow pattern, information entropy, recurrence chart

带肋矩形直通道内的冷却空气换热特性研究 = **Study of the Heat Exchange Characteristics of the Cooling Air Inside a Straight Ribbed Rectangular Channel** [刊 汉] LIU Rui, SHUI Lin-qi, WANG Xin-jun, BAI Xiao-wei (Turbo-machinery Research Institute, Xi'an Jiaotong University, Xi'an, China, Post Code: 710049) // Journal of Engineering for Thermal Energy & Power. - 2011, 26(5). - 543 ~ 546

By using the commercial software ANSYS CFS , numerically calculated were the heat exchange characteristics of the cooling air inside a straight ribbed rectangular channel and compared were the calculation results with the test data obtained by Han. Furthermore ,the influence of Reynolds and the angle of ribs on Nusselt number was also analyzed. It has been found that the average Nusselt number obtained from the numerical calculation assumes an identical variation tendency to the test values. The calculation results ,however ,were bigger than the test values. Due to the flow disturbance role played by the ribs ,two vortexes will be produced in the zone between any two ribs ,enhancing the heat exchange between the cooling air and the solid wall surfaces. With an increase of Reynolds and Nusselt number , the average friction resistance coefficient will also increase. When the angle of ribs falls in a range from 45 to 60 degrees , the intensified convection heat exchange effectiveness in the cooling channel is assessed as the best.

**Key words:** blade cooling , rectangular channel , flow and heat exchange

以水为工质的 EHD 强化管内对流换热实验研究 = **Experimental Study of the Electrohydrodynamically ( EHD) -intensified Convection Heat Exchange Inside a Tube With Water Serving as the Working Medium**

[刊 汉] YANG Xia , ZHANG Jie , WU Yan-yang , ZHANG Tao ( College of Electromechanical Engineering , Wuhan Engineering University , Wuhan , China , Post Code: 430073) // Journal of Engineering for Thermal Energy & Power. - 2011 , 26( 5) . - 547 ~ 550

With water serving as the working medium , experimentally studied was the EHD ( electrohydrodynamics) intensification mechanism controlling the convection heat exchange inside water jacket heat exchanger tubes. During the test , a direct current type high voltage electrode was mounted at the center of the water jacket heat exchanger tubes and the voltage of the electrode was within a range from DC 0 ~ 40 kV. A total of five groups of combined intensification test were performed at different flow rates and voltages respectively. The test results show that under the condition of different flow rates inside the tubes , the electric field all played intensification role to various extents on the heat conduction process inside the tubes. When the flow rate is  $0.1 \text{ m}^3/\text{h}$  , the intensification coefficient of the electric field  $\theta$  attains its maximal value , being up to 1.224. When the flow rate is  $1.0 \text{ m}^3/\text{h}$  , the above-mentioned coefficient  $\theta$  attains its minimal value , verifying that the electric field plays an intensification role on the convection heat conduction process with water serving as the working medium. It has also been found , however , that the intensification effectiveness achieved by the electric field enjoys a specific feature , which is susceptible to any change of the flow rate and at an identical flow rate , there exists an optimum intensification voltage value. It is not true that the higher the voltage value the better the intensification effectiveness. **Key words:** electrohydrodynamics ( EHD) , convection heat exchange , intensified heat transfer , electric field

航空煤油在微通道中传热性能的实验研究 = **Experimental Study of the Heat Transfer Performance of Aviation Kerosene in Microchannels**

[刊 汉] CHEN Hai-gang , HUANG Yong , MIAO Hui ( Key Laboratory on Aero-engine Aerodynamics and Thermodynamics , College of Energy Source and Power Engineering , Beijing University of Aeronautics and Astronautics , Beijing , China , Post Code: 100191) // Journal of Engineering for Thermal Energy